Water quality modeling of a eutrophic drinking water source: Impact of future climate on Cyanobacterial blooms

Citation for the original published paper (version of record):
Elhabashy, A., Li, J., Sokolova, E. (2023). Water quality modeling of a eutrophic drinking water source: Impact of future climate on
Cyanobacterial blooms. Ecological Modelling, 477.
http://dx.doi.org/10.1016/j.ecolmodel.2023.110275

Ecological Modelling 477 (2023) 110275

Contents lists available at ScienceDirect

Ecological Modelling

journal homepage: www.elsevier.com/locate/ecolmodel

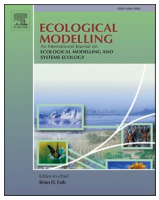

Water quality modeling of a eutrophic drinking water source: Impact of future climate on Cyanobacterial blooms

Ahmed Elhabashy [a,b], Jing Li [c], Ekaterina Sokolova [a,b,*]

[a] Department of Architecture and Civil Engineering, Chalmers University of Technology, Gothenburg, Sweden
[b] Department of Earth Sciences, Uppsala University, Uppsala, Sweden
[c] Water Resources Engineering, Department of Building and Environmental Technology, Lund University, Lund, Sweden

ARTICLE INFO

Keywords:
Blue-green algae
Chlorophyll-a
Climate change
Hydrodynamic model
Nutrient loading
Process-based modeling

ABSTRACT

Cyanobacterial blooms are becoming more frequent in freshwater sources, causing concern throughout the world. Cyanobacterial blooms affect human health and the entire environment. Numerical modeling is an effective tool for investigating aquatic systems. In this study, a 3D hydrodynamic and water quality (ecological) model was used to simulate eutrophication of a drinking water source, Lake Vomb, in Sweden under present and future scenarios. The hydrodynamic model was set-up in MIKE 3 FM software based on meteorological, hydrological, and water quality data. The hydrodynamic model performance was satisfactory in terms of the water temperature simulation, with root-mean-square-error (RMSE) ranging from 0.38 to 1.2 °C. In the ecological model, Chlorophyll-a (Chl-a) was used as a proxy for Cyanobacteria, and the model proved acceptable in simulating the Chl-a concentrations, with a Nash-Sutcliffe efficiency (NSE) of 0.93 and 0.87 for calibration and validation respectively. The findings revealed that external nitrogen loading and internal phosphorus loading had significant impact on the nutrient concentrations in Lake Vomb. The findings also showed a correlation between Chl-a levels and total phosphorus levels in the lake. To simulate future water quality in the lake, two Representative Concentration Pathways (RCP) for the year 2050 were used to make projections for changes in air temperature and precipitation. Under the projected future climate, the simulations showed a considerable rise in Cyanobacteria biomass independent of the changes in external nutrient loading. The model findings can assist water managers in planning mitigation strategies by identifying major nutrient sources.

1. Introduction

Cyanobacteria (often called blue-green algae) are microscopic organisms that can form dense, slimy, and sometimes toxic blooms in the aquatic environments (Huisman et al., 2018). The release of cyanotoxins has the potential to endanger the ecosystem as well as the human health. Toxin production by Cyanobacterial blooms varies in space and time (Huisman et al., 2018). Some toxins are released into the water after cell death; however, some Cyanobacteria species release toxins without cell death or rupture. Some toxins can harm the liver, while others can be lethal, such as Anatoxin-a, which causes death via neural damage within minutes (Méjean et al., 2014). Cyanobacteria thrive in environments where light, water, and nutrients (mostly nitrogen and phosphorus) are abundant (Chorus and Welker 2021). Cyanobacterial blooms in lakes are associated with the overgrowth under eutrophication with high nutrient loadings into water bodies (Conley et al., 2009). These blooms can form immediately at the surface and cover large areas of the water body and are most common in the upper layers where light is accessible for photosynthesis, but may form deeper inside the water column as well (Huisman et al., 2018). These blooms are increasing both in frequency and magnitude across the globe and pose challenges to freshwater systems ranging from aesthetics to serious human health risks (Huisman et al., 2018).

Cyanobacterial blooms are known to be positively correlated to the total phosphorus (TP) levels in water bodies, and therefore phosphorus is often the limiting factor for growth (Xie et al., 2011; Li et al., 2018; Payen et al., 2021). Excess TP in freshwater is linked to agricultural and urban growth (Paerl and Barnard 2020) and is caused by, for example, manure in grazing grounds and fertilizer use in agricultural fields (Motew et al., 2017), as well as effluents from wastewater treatment facilities (Comber et al., 2015). Over time, TP accumulates in lake sediments and can be resuspended and mixed in the water column; this

* Corresponding author.
E-mail address: ekaterina.sokolova@geo.uu.se (E. Sokolova).

https://doi.org/10.1016/j.ecolmodel.2023.110275
Received 7 November 2022; Received in revised form 29 December 2022; Accepted 4 January 2023
Available online 11 January 2023

process is usually referred to as internal loading. On the other hand, nitrogen can be a co-limiting factor for algal growth. Some Cyanobacteria species can fix atmospheric nitrogen, allowing them to grow even when nitrogen levels are low in the water (Li et al., 2018; Chorus and Welker 2021). In addition to nitrogen fixation, Cyanobacteria can uptake inorganic nitrogen (IN) from the water column for growth. Similar to TP, high IN levels in water bodies originate from anthropogenic activities such as the use of fertilizers in agriculture, wastewater effluents, or nitrogen oxides emissions from industrial development (Erisman et al., 2013).

Deterioration of Swedish waters due to eutrophication has been investigated since the second half of the 20th century (Willén 1972), and phytoplankton has been considered an important water quality variable since 1964 (Willén 2001). The investigations were mainly focused on large lakes (e.g., Lake Mälaren and Lake Vättern) near highly populated areas. The knowledge of phytoplankton before 1965 was limited; thus, these investigation projects were vital for assessment and future comparison. The blue-green algae were noticed to predominate in 1969–1970 in Lake Mälaren corresponding to extremely hot summers (Willén 1972). Reports of early sight of algal blooms were even found in the 1940s in Lake Ringsjön with the first known algal poisoning in 1968 (Cronberg et al., 1999). Over time, Cyanobacteria biomass were increasing even in nutrient-poor lakes under global warming. In their study of many nutrient-poor lakes in southern Sweden, Freeman et al. (2020) found a relative increase in Cyanobacteria biomass of 21% between the years 1998–2013.

Climate change effects have been globally seen in higher air temperatures, severe precipitation events, and altered hydrological cycles (Taranu et al., 2015; Meerhoff et al., 2022). Cyanobacterial proliferation can be affected by climate change in both direct and indirect ways. Warmer climate conditions result in increase in surface water temperature (Piccolroaz et al., 2020) that can directly accelerate in-lake biochemical processes and in turn increase phytoplankton biomass (Thomas et al., 2017). Climate change can also influence nutrient loading by altering the hydrological and nutrient cycles affecting algal growth (Meerhoff et al., 2022). Kakouei et al. (2021) studied the impacts of changes in climate and land use on over 1500 lakes in Europe and North America and concluded that Cyanobacteria abundance is expected to increase with the increase in temperature and radiation with a decrease in wind speed and forest areas under urbanization. In Sweden, both the average precipitation and air temperature are projected to increase under climate change scenarios (Jiménez-Navarro et al., 2021).

Modeling of Cyanobacteria has a long history dating back to the early 20th century when scientists first began studying these organisms in detail. In the 1950s and 1960s, researchers developed simple models to understand the basic biology and ecology of Cyanobacteria. These models focused on the role of Cyanobacteria in nutrient cycling and the factors that influence their growth and distribution. In the 1980s and 1990s, advances in computer technology and computational biology allowed for the development of more complex models that took into account a wider range of biological processes and environmental factors and were used to better understand the role of Cyanobacteria in ecosystems and to predict their responses to environmental changes (Guven and Howard 2006). Process-based modeling of aquatic ecosystems simulates the interaction between the complex physical, biological, and chemical processes (Anagnostou et al., 2017). Models vary intrinsically in their formulae, level of detail, simplicity, and applicability; however, all eutrophication models include the fate and transport of nutrients, dissolved oxygen dynamics, and temperature dependency of their processes (Anagnostou et al., 2017; Vinçon-Leite and Casenave 2019). Multiple eutrophication modeling studies (e.g., Elliott et al., 2007; Markensten et al., 2010; Trolle et al., 2011; Elliott and Defew 2012; Tasnim et al., 2021) utilized Chlorophyll-a (Chl-a) as a proxy for Cyanobacteria biomass in lakes and rivers. Since Chl-a is an indication of all phytoplankton species, many models predict total phytoplankton biomass with the premise that Cyanobacteria dominate the growth (Vinçon-Leite and Casenave 2019). Several studies have investigated the effects of climate change on algal blooms (e.g., Markensten et al., 2010; Trolle et al., 2011; Yindong et al., 2021). Trolle et al. (2011), in their study area in New Zealand, found that future warmer air temperature can impact eutrophication equivalent to increasing external nutrient loading by up to 50%. Although predicted climate change impacts vary in magnitude and duration, most of the models predict more intense blooming under future warming conditions (Yindong et al., 2021).

The goal of this study was to apply a hydrodynamic and water quality model to investigate mixing dynamics, in-lake nutrient dynamics, and Cyanobacterial bloom developments under present and future conditions in a drinking water source (Lake Vomb) in Sweden. The results of this study benefit the safety of the local drinking water supply and are useful for other temperate and eutrophic lakes. A 3D hydrodynamic model of the lake was created using MIKE 3 FM (Powered by DHI) and calibrated to describe the water temperature distribution in the lake. Then, a 3D ecological model was calibrated to simulate Chl-a as a surrogate for Cyanobacteria in the lake. The research questions that this study addresses are:

- How accurate can a 3D model with an intermediate level of detail describe eutrophication conditions?
- What are the driving forces of algal blooms in Lake Vomb?
- How will the future changes in temperature and precipitation affect the future algal blooms in Lake Vomb?

2. Materials and methods

2.1. Study area

Lake Vomb (55° 41′ N, 13° 35′ E) is a freshwater lake in Scania, Sweden's southernmost region (Fig. 1). Lake Vomb has a surface area of around 12 km^2 and an average depth of 6.6 m with a maximum depth of 16 m. The lake serves as a drinking water source to approximately 350 000 people in Malmö, parts of Lund, and other parts of Scania. Lake Vomb is located in Kävlingeån's catchment with agriculture as the dominating land use and has three main tributaries, namely Björkaån, Torpsbäcken, and Borstbäcken. The water quality in the lake suffers from heavy nutrient loading through runoff from agricultural lands as well as wastewater effluents (Bergion et al., 2018; Li et al., 2018; Chuquimia et al., 2019). As a result, heavy algal blooms have been observed in the lake for decades with Cyanobacteria frequently dominating the algal blooms (Li et al., 2018). The most common species of Cyanobacteria are *Microcystis* spp. (Johansson et al., 2019).

2.2. Model input data

The model was set-up and calibrated on the year 2019 (baseline) and validated on the year 2020. The data required to set up the model included water temperature measurements used for calibration and validation, lake bathymetry data (provided by Sydvatten AB), hydrological and water quality data for the tributaries, and meteorological conditions.

The hydrodynamic model was calibrated and validated using the water temperature data from the lake profile monitoring program at Lake Vomb by Sydvatten AB. The data were measured at six locations (Fig. 1) in the lake with 1 m vertical resolution from the surface to the bottom of the lake. The temporal resolution of the data varied with season, from almost no data in winter to ten monitoring occasions per month in summer.

The hydrological data for the three tributaries to the lake, Björkaån, Torpsbäcken, and Borstbäcken, were daily time-series of discharge and water temperature downloaded from the Swedish Meteorological and Hydrological Institute (SMHI) modeled data webpage (https://vattenwebb.smhi.se/modelarea/) for the years 2019 and 2020. The water level at the lake outlet was used as a boundary condition, and the

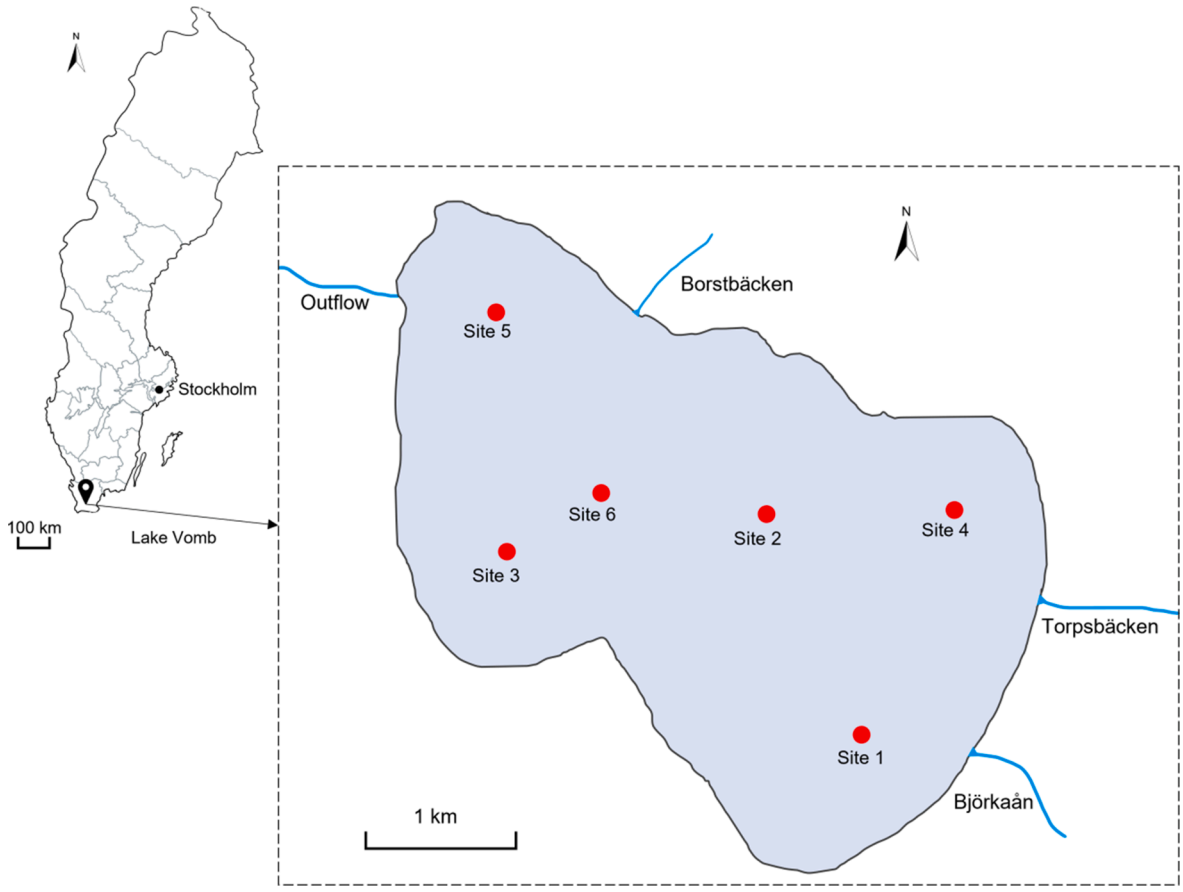

Fig. 1. Lake Vomb study area with sampling sites (red circles) and inflow tributaries (Björkaån, Torpsbäcken, and Borstbäcken); a web version of the study area can be found at: https://www.google.com/maps/d/edit?mid=1eqoEwQpNg4EtuP2_tnz-1npRMO1bg3mb&usp=sharing.

data were obtained from the reports of Kävlingeån's water council for the years 2019 and 2020 (Ekologigruppen Ekoplan AB 2020, 2021). A constant extraction of 1 m^3/s was included in the model to account for the water withdrawal for drinking water production.

The meteorological data used in the model were downloaded from SMHI for the years 2019 and 2020. The data for precipitation were obtained with daily resolution from the Vomb station (reference number 53410). The data for wind speed and direction, air temperature, and relative humidity were obtained with hourly resolution from the Hörby A station (53530), which is located around 20.5 kms north of Lake Vomb. Furthermore, the data for hourly shortwave radiation were obtained from the Lund station (53445), which is approximately 23 kms west of the lake, and hourly longwave radiation data were only accessible at the Växjö station (64565), which is more than 100 kms north. The future projections for air temperature and precipitation were downloaded from SMHI's Advanced Climate Change Scenario Service (https://www.smhi.se/en/climate/future-climate/advanced-climate-change-scenario-service/met/skane_lan/medeltemperatur/rcp45/2041–2070/year/anom) for Scania County for the period between 2041–2070 in the form of seasonal changes compared to a reference period 1971–2000. The year 2050 was chosen as the target year under two Representative Concentration Pathway (RCP) scenarios, namely RCP4.5 and RCP8.5. The RCPs depict scenarios for climate modeling and are labelled after possible future total solar radiative forcing by the year 2100 resulting from greenhouse gas emission. RCP4.5 (4.5 W/m^2) is a moderate scenario in which emissions peak around the year 2040 and subsequently drop, while the highest emissions scenario, RCP8.5 (8.5 W/m^2), assumes emissions will continue to rise throughout the century. As a result, climate change under RCP8.5 is expected to be more severe than under RCP4.5. We limit the future projections in this study to air temperature and precipitation. In addition to the data utilized for the baseline year 2019, the historical records of air temperature were obtained for numerous sites in Scania County, i.e., SMHI stations 52230, 53300, 53430, 53530, 54230, 54290, 62030, and 62040, to cover as much of the county's geographical expanse as possible. These data were used to calculate seasonal average temperatures in the periods 1971–2000 and 2015–2019 (the five-year period was deemed more representative than the single year 2019) to adjust the expected changes reported by SMHI with the changes that had already occurred up until 2019. Likewise, the historical records for precipitation were obtained from SMHI stations 52230, 53260, 53290, 53320, 53410, 53500, 53540, 54290, 62120, and 63080, and the changes in seasonal average precipitation (in mm/month) projected by SMHI were then adjusted with the changes that had previously occurred between the reference period 1971–2000 and 2015–2019. The expected changes in 2050 were then expressed as a percentage increase over the baseline year 2019. To create input data for the year 2050 under RCP4.5 and RCP8.5 scenarios, the data-series for air temperature and precipitation of the year 2019 were adjusted with projected seasonal changes as shown in Section 1 in the supplementary document.

The water quality data were downloaded from the reports produced by Kävlingeån's water council (Kävlingeåns Vattenråd) for the years 2019 and 2020 (Ekologigruppen Ekoplan AB 2020, 2021) and from the database of the Swedish University of Agricultural Sciences (SLU) for lakes and watercourses (https://miljodata.slu.se/mvm/). The following data were extracted and combined from both datasets: biochemical oxygen demand (BOD), ammonium (NH_4), nitrite (NO_2), nitrate (NO_3), TP, and dissolved oxygen (DO) in the three tributaries (Björkaån, Torpsbäcken, and Borstbäcken). The water quality data were available from April to December in both the calibration year 2019 and validation

year 2020. The temporal resolution of the data was approximately monthly; therefore, linear interpolation was conducted to deduce daily concentrations of all the variables. The model simulations were compared to the observation data for these variables (except for BOD due to unavailability) at one location in the lake; the data were downloaded from SLU in the surface and bottom layer. Chl-a measurements were only available from SLU for the surface layer at the same location in the lake; SLU uses a spectrophotometer in accordance with Swedish standards (SS 22028146). All other variables were measured by SLU or Kävlingen's water council in accordance with Swedish/European standards (Ekologigruppen Ekoplan AB 2020, 2021).

The modeling results for Chl-a were compared to additional measurements from satellite (Sentinel-3) data provided by DiCyano project partner, Brockmann Geomatics Sweden AB. Sentinel-3A and 3B are observation satellites within the Copernicus program launched on 16 February 2016 and 25 April 2018 respectively. Chl-a levels in the surface water were extracted from all available images during 2016–2021 and used for the comparison with respective simulated years. All estimates were calculated as a mean of all valid (e.g., cloud free) pixels (9 at maximum) centered on the predefined station coordinate; the pixels are 300 × 300 m in size.

2.3. Model description

MIKE 3 FM (powered by DHI https://www.mikepoweredbydhi.com/products/mike-21–3) was used in this study for hydrodynamic and water quality modeling. MIKE 3 FM is based on the flexible mesh approach, which employs a cell-centered finite volume method to solve the Navier-Stokes equation for incompressible fluids in its Reynolds averaged form. The module's governing equations are the shallow water equations, which are simplified Navier-Stokes equations. The computational mesh for Lake Vomb was created using the point elevations of the lake's bottom. The mesh was composed of 536 nodes and 935 triangular mesh elements with areas ranging from 2150 to 30 839 m^2. Vertically, the lake was divided into 16 layers, two of which were set up using sigma coordinates (upper 1 m of the lake) and the others (of 1 m height each) using Cartesian z-coordinates. The water density in the model was defined as a function of temperature. Bed resistance roughness height and wind friction coefficient were set to model default values of 0.05 m and 0.00125, respectively. The horizontal and vertical eddy viscosities were simulated using Smagorinsky and k-epsilon formulations, respectively, using model default settings. Heat exchange between the water and the atmosphere was included in the model and contained latent heat, sensible heat, short and long wave radiation, as well as atmospheric conditions for air temperature and relative humidity. The hydrodynamic simulations spanned the period January-December of each year, whereas the water quality simulations covered April-December due to data availability. The initial conditions of water level, water temperature, and the water quality state variables were set to match the measurements in the lake on the corresponding simulation start dates.

The water quality model was adapted by modifying the *MIKE 21/3 WQ with nutrients and chlorophyll-a* template in the ECO Lab module. The template included the interdependent state variables: BOD, DO, TP, IN, and Chl-a. The model equations applied similar principles to other models, such as accounting for light and temperature dependency. The key distinction between the model equations and other models is that the stoichiometry of the photosynthetic process is used to calculate Chl-a growth rather than an empirical growth parameter. The full set of model equations and the calibrated parameter values can be found in the supplementary document (Section 2). The following is a brief overview of the main processes. In ECO Lab, each state variable is affected by the advection-dispersion and is also defined by an ordinary differential equation that models its rate of change under the applicable processes. The scaled eddy viscosity formulation was used to apply the dispersion in the model; the horizontal scaled constant was set to 1 for all the variables, whereas the vertical constant was 0.1 except for DO which was calibrated to 0.001. In the selected template, Chl-a production is modeled proportional to the net daily oxygen production. The template was modified from default to include phosphorus release from sediment (internal loading) and temperature dependency of Chl-a growth. To characterize the nutrient constraints for development, the Michaelis-Menten equation with half-saturation constants were utilized. To account for the temperature effect, the Arrhenius formula was used. The IN cycle in the model was simulated in terms of NH_4, NO_2, and NO_3 components and included the yield from BOD decay, uptake by plants and bacteria, nitrification, and denitrification processes. The TP cycle included the yield from BOD decay, uptake by plants and bacteria, and sediment release. The TP sediment release mechanism was included as temperature dependent, and the effect of bottom layer DO levels on the release was accounted for by multiplying by the inverse of Michaelis-Menten formula. Lastly, the DO variable included the net photosynthetic oxygen production, reaeration with the atmosphere, nitrification, BOD decay, and sediment oxygen demand. The net photosynthetic oxygen production is computed by subtracting phytoplankton respiration from light-dependent photosynthesis.

In this study, the root-mean-square-error (RMSE) and Nash-Sutcliffe efficiency (NSE) coefficients were utilized as statistical performance metrics. The standard deviation of the prediction errors is represented by the RMSE (Eq. (1)). The NSE (Eq. (2)) computes a dimensionless number in the range $\{-\infty, 1\}$ where NSE = 1 indicates a perfect match, NSE = 0 indicates that the model performance is equivalent to assuming the mean actual value, and NSE < 0 indicates that the model fails to perform better than simply assuming the mean value.

$$RMSE = \sqrt{\frac{\sum_i^N (Prediction_i - Actual_i)^2}{N}} \tag{1}$$

$$NSE = 1 - \frac{\sum_i^N (Prediction_i - Actual_i)^2}{\sum_i^N (Actual_i - Mean\ Actual)^2} \tag{2}$$

3. Results

3.1. Model evaluation and temporal variations of state variables

To calibrate the hydrodynamic model using water temperature measurements of the year 2019, the values for the heat exchange parameters, namely light extinction coefficient, heating coefficient, and cooling coefficient, were adjusted, and the final values were 0.45 (1/m), 0.009, and 0.009, respectively. The model was then validated using the water temperature data of the year 2020. The simulated and measured water temperature time-series for the six sites can be found in the interactive Supplementary Figures T1 to T6. The simulated water temperatures from the model were retrieved to compare with the available data from the six observation sites, and the RMSE and NSE were determined for each depth at each site. The modeling results of water temperature for the calibration year 2019 demonstrated close agreement at all measurement locations (Table 1). Similarly, the modeling results for water temperature for the validation year 2020 were in fair agreement with the measured data, except for several instances when bottom layer temperature was underestimated. The simulations of water temperatures indicated that the lake mixes continuously throughout the year. During the summer season, particularly during the first three weeks of June, the temperature gradient with depth occasionally resembled stratification conditions at the lake's deepest point (site 2, Supplementary Figure T2), but the gradient was not strong enough (less than 1 °C/m) to be classified as thermal stratification.

Similar to the hydrodynamic model, the water quality model was calibrated using the observations of the year 2019 to determine the model parameters, and the model was then validated using the data of the year 2020. Among all the modeled water quality variables, the

Table 1
Model performance metrics during calibration (year 2019) and validation (year 2020) for the surface and bottom layers of the lake.

Variable	Surface Layer				Bottom Layer			
	RMSE		NSE		RMSE		NSE	
	2019	2020	2019	2020	2019	2020	2019	2020
Temperature[1]	0.38–0.44 °C	0.42–1.2 °C	0.94–0.99	0.94–0.98	-	–	–	–
Inorganic nitrogen	284 μg/l	211 μg/l	0.98	0.99	247 μg/l	267 μg/l	0.98	0.97
Total phosphorus	14.7 μg/l	31.0 μg/l	0.91	0.55	34.0 μg/l	35.9 μg/l	0.55	0.50
Dissolved oxygen	1.52 mg/l	2.22 mg/l	0.69	0.34	1.62 mg/l	1.84 mg/l	0.91	0.88
Chlorophyll-a[2]	8.28 μg/l	12.1 μg/l	0.93	0.87	–	–	–	–

[1] Values represent the ranges from all measurement sites and are averaged across multiple depths.
[2] Values were calculated based only on the measurements from SLU.

simulated IN had the best agreement with the measurements (Table 1, Fig. 2). The high seasonal variability of surface IN concentrations found in both model results and measured data (Fig. 2) clearly demonstrates the influence of nitrogen provided by the external loading. In the spring, the tributaries discharge a significant load of IN which is reduced during the summer.

In contrast, the input from the tributaries was shown to have minimal impact on the peak in TP concentrations in autumn 2019, and the major contributor to TP was found to be the internal loading. The sediment release rate of TP at 20 °C was calibrated to 20.5 mg/m^2/d and varied with temperature and DO content. The addition of the DO influence on the sediment release of TP enhanced model performance, since TP concentrations were seen to increase following incidences of decreased bottom DO concentrations (Fig. 2). The statistical measures (Table 1) and the visual assessment of the findings (Fig. 2) showed that the model follows the overall trend of TP.

The modeling results for surface DO showed general agreement with the observations, but failed to reflect fine local fluctuations in the surface DO levels and instead fell within the season's average, but the modeling results for the bottom layer showed better agreement with observations (Table 1, Fig. 2). It was critical that the model captures the events of low DO bottom concentrations (e.g., end of July and start of August 2019; Fig. 2) in order to accurately apply their impact on the sediment release of TP. Lastly, the simulated concentrations of surface DO were seen to be negatively correlated to Chl-a.

Chl-a simulations were in agreement with the general pattern of observations from SLU (Table 1, Fig. 3); however, the satellite deduced Chl-a levels suggested high variability in the summer blooms (Fig. 3). The mortality and settling rates, and the growth temperature coefficient of Chl-a were calibrated. To account for the link between TP and Chl-a, the nutrient limitation function in the model was adjusted. The nutrient limitation function was calibrated to also reduce the nitrogen limitation on Chl-a growth. Chl-a concentrations in the lake increased during late spring and peaked at late summer with concentrations more than 20 μg/l (Fig. 3).

3.2. Effects of climate change on the lake

The simulated future scenarios showed a rise in water temperature that was proportional to the expected air temperature. The simulated water temperature time-series at the deepest section of the lake (site 2) can be found in Supplementary Figure T7. In 2050, the average annual rise in water temperature was +0.665 °C under RCP4.5 and +1.043 °C under RCP8.5 scenarios, relative to the baseline scenario. Summer, autumn, and winter changes were more dramatic than spring changes (Table 2). The days with a substantial water temperature gradient in the

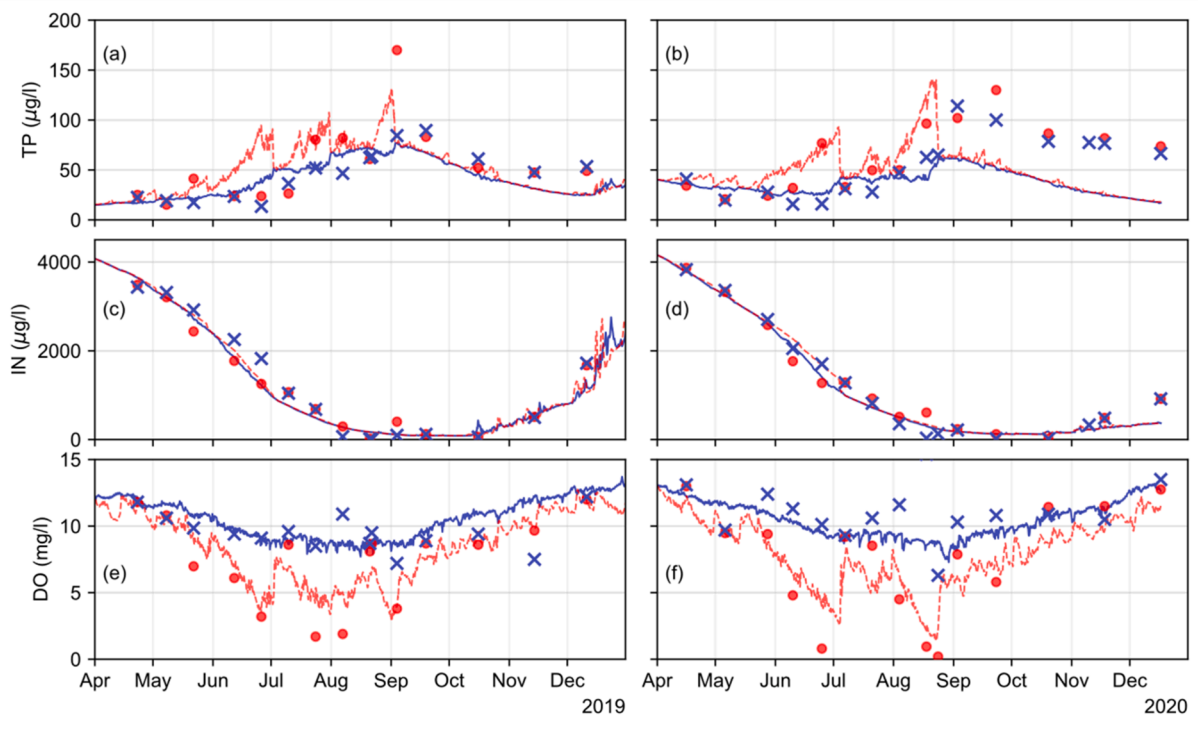

Fig. 2. Simulations (lines) and measurements (scatter) of a-b) total phosphorus (TP), c-d) inorganic nitrogen (IN), and e-f) dissolved oxygen (DO) at the lake surface (blue) and bottom (red) layers in Lake Vomb in the calibration year 2019 (left) and the validation year 2020 (right).

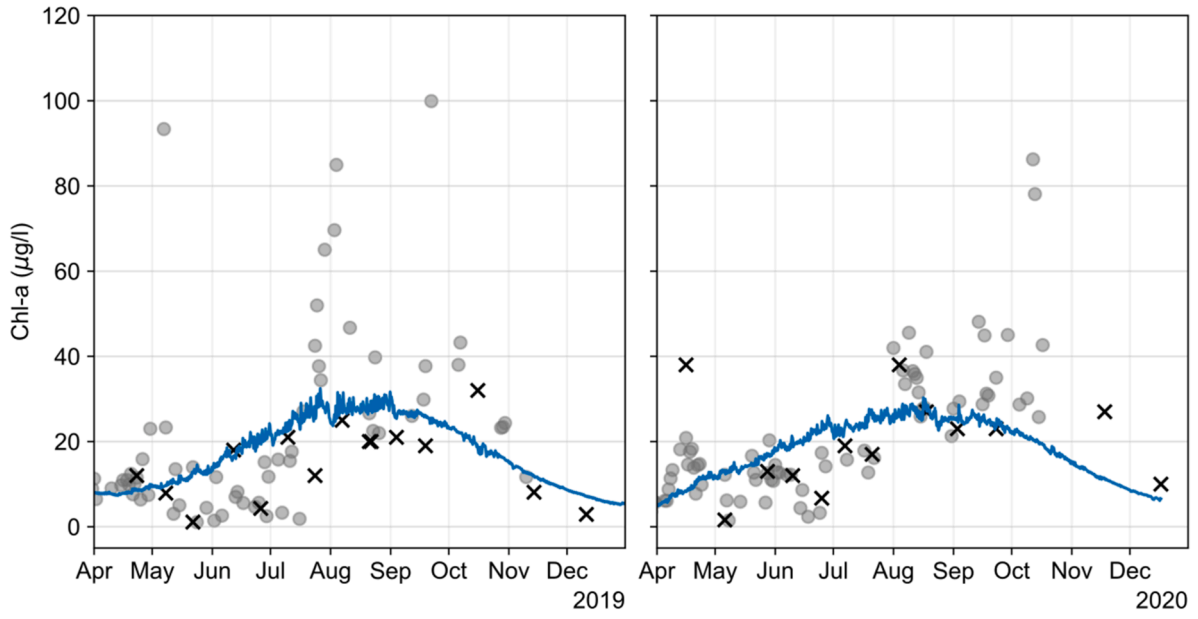

Fig. 3. Chlorophyll-a (Chl-a) concentrations in the calibration year 2019 (left) and the validation year 2020 (right) at the lake surface in the center of Lake Vomb: simulations (line) compared to measurements from SLU (crosses) and Satellite (circles).

Table 2
Seasonal projected changes in state variables at the surface of Lake Vomb under future scenarios compared to the baseline year 2019.

Variable	Winter		Spring		Summer		Autumn	
	RCP4.5	RCP8.5	RCP4.5	RCP8.5	RCP4.5	RCP8.5	RCP4.5	RCP8.5
Δ Water temperature (°C) [1]	+0.77	+1.07	+0.43	+0.76	+0.68	+1.0	+0.78	+1.26
Δ Chlorophyll-a (%)	+7.58	+11.8	+1.74	+3.15	+2.76	+4.24	+5.32	+7.90
Δ Total phosphorus (%)	+12.1	+19.9	+2.00	+3.70	+8.74	+14.0	+18.9	+30.2
Δ Inorganic nitrogen (%)	-1.96	-2.88	-1.36	-2.48	-15.6	-23.3	-15.4	-21.4
Δ Dissolved oxygen (%)	-2.61	-3.72	-1.07	-1.91	-1.91	-2.88	-2.27	-3.51

[1] Averaged across multiple depths.

baseline simulation, exhibited a stronger gradient in the future scenarios (Section 3, supplementary document).

Increased lake water temperatures accelerated the temperature-dependent water quality processes in the model. In comparison to the baseline year 2019, Chl-a surface levels under climate change scenarios RCP4.5 and RCP8.5 increased in all seasons, and this increase was most pronounced in fall and winter (Table 2, Fig. 4). This increase in Chl-a levels was caused by the increase in TP together with the increased water temperature. Similarly, TP levels increased over the summer, autumn, and winter (Fig. 4). This was a direct effect of the lake's internal loading mechanism, which is temperature dependent. In contrast, the concentrations of IN and DO decreased under both scenarios (Fig. 4). This was expected since the IN levels of the baseline year were strongly controlled by external loading; thus, the higher temperature accelerated the nitrogen processes (e.g., denitrification) while the external loading remained unchanged.

4. Discussion

MIKE 3 FM was used in this study to model the hydrodynamics and ecological conditions of the eutrophic Lake Vomb. The model was created and calibrated for the year 2019 and validated on the year 2020. The model performance was satisfactory in representing all state variables (Table 1). To investigate the impact of projected changes in air temperature and precipitation for the year 2050, RCP4.5 and RCP8.5 were chosen as medium and severe scenario, respectively. For simplicity, other input to the model (e.g., solar radiation, wind, and relative humidity) remained unchanged between scenarios. The future scenarios showed a projected increase in Cyanobacteria biomass (Table 2).

Throughout the baseline year 2019, the simulated and measured water temperature indicated no obvious thermal stratification conditions in Lake Vomb, i.e., the temperature gradient in the water column was always less than 1 °C/m. To investigate this behavior, the mixing depth was calculated using the empirical equation: $(10^{0.185\log(A)+0.842} - 2.37)/1.05$, where A is the lake surface area in km^2 (Qin et al., 2020). The lake's mixing depth was estimated to be 8.2 m, which is more than the lake's average depth of 6.6 m, explaining the lake's unlikelihood of stable thermal stratification. In the future scenarios, the projected rise in air temperature caused an increase in water temperature, however precipitation had essentially little effect on simulated water temperature. Interestingly, the increase in water temperature was rather uniform across the water column, with a similar shape of the temperature profiles to the ones from the baseline year 2019. This was mostly due to the solar radiation and wind conditions, which were kept the same in the model for the future scenarios as in the baseline. However, water temperature changes were not uniform in the summer season, and future projections appeared to favor larger thermal gradients. Using observed solar radiation conditions improved the simulation of the lake hydrodynamics. The errors in the simulated temperatures can stem from the manual calibration of the multivariate model parameters (Li et al., 2017), as well as uncertainty in meteorological data due to errors in measurements or the absence of some data in the lake's immediate vicinity.

The modeling results for TP showed that when only external

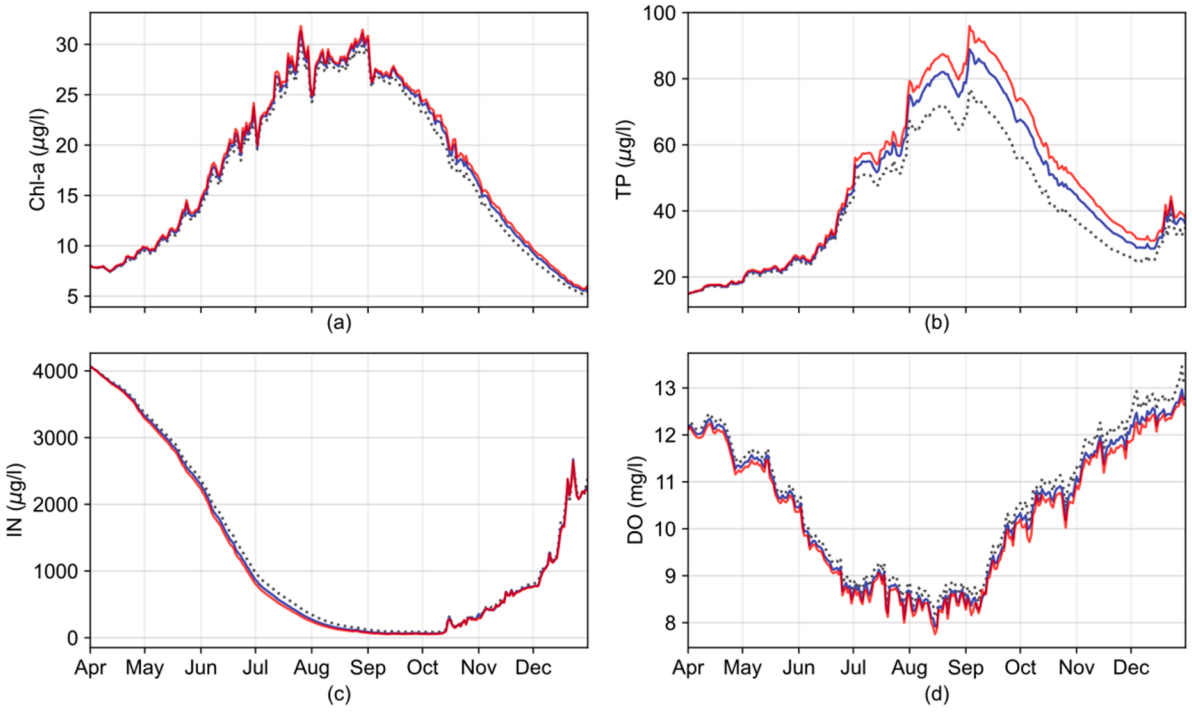

Fig. 4. Simulations of a) Chlorophyll-a (Chl-a), b) total phosphorus (TP), c) inorganic nitrogen (IN), and d) dissolved oxygen (DO) at the lake surface for the baseline year 2019 (black; dotted) and 2050 scenarios RCP4.5 (blue) and RCP8.5 (red).

phosphorus loading was considered, the TP levels in the lake were significantly lower than those observed. The internal loading mechanism improved the model performance and allowed the model to reproduce the autumn TP peaks (Fig. 2). This finding is consistent with the findings of Qin et al. (2020), who showed that shallow and medium lakes have considerable interaction between the sediments and water column, influencing nutrient dynamics. The release of TP from sediments was modeled as temperature-dependent, according to the findings of several studies (Redshaw et al., 1990; Wu et al., 2014). Consequently, under warmer future conditions, higher TP levels were projected (Fig. 4); this increase can be expected since warmer temperatures affect phosphorus adsorption to sediments (Cornelissen et al., 1997) and enhance the exchange with the overlaying layers. Additionally, the inclusion of DO impact on the release mechanism slightly improved TP simulations. Furthermore, for simplicity and data availability, this study employed TP as the limiting nutrient of Cyanobacteria. While this method is commonly employed in research (Trolle et al., 2008; Chen et al., 2013; Huang et al., 2015; Cui et al., 2016), using TP remains a simplification since only a fraction of TP (e.g., soluble reactive phosphate) is available for Cyanobacteria uptake (Chorus and Welker 2021). In contrast to TP, the IN levels in the lake were shown to be controlled by the mass flow from the tributaries, rendering in-lake nitrogen generation insignificant. The lake receives elevated nitrogen loading over the winter to early spring, as seen in the two modeled years 2019 and 2020 (Fig. 2). The model results showed exceptional agreement with observed IN for both the surface and bottom layers in the lake (Table 1).

To account for the capacity of Cyanobacteria to fix nitrogen from the atmosphere, the effect of IN limitation on the Chl-a growth process in the model was lessened. Thus, Chl-a levels in the lake were observed to rise even when overall nitrogen concentrations decreased (given an increase in TP). The model findings demonstrated that Chl-a levels are positively correlated with TP; this is consistent with previous research studies that emphasize phosphorus as the most significant limiting nutrient (Xie et al., 2011; Schindler et al., 2016; Li et al., 2018; Payen et al., 2021). According to sensitivity analysis, TP internal loading had the major impact on Chl-a levels (Section 4, supplementary document). On the other hand, Chl-a was also noticed to be negatively correlated with IN (Fig. 2 and Fig. 3), but this was attributed to the seasonal variation of IN mass flow from the tributaries. Under future conditions, the biomass of Cyanobacteria (represented by Chl-a concentration) was shown to increase even without any increase of nutrient loadings from the catchment. Higher Chl-a concentrations were found in all seasons because of increased lake temperatures as well as the increase in TP content in the lake from internal loading. Because of the lower Chl-a levels in winter and autumn in the baseline scenario, the relative seasonal rise in Chl-a was more pronounced in these seasons compared to spring and summer (Table 2). In general, this projected increase was consistent with other research on the influence of climate change on Cyanobacterial proliferation in another part of Sweden (Markensten et al., 2010), New Zealand (Trolle et al., 2011), and China (Yindong et al., 2021).

To the best of our knowledge, this study is the first attempt to model nutrients and Cyanobacteria conditions in Lake Vomb. Moreover, this study reports a further development of water quality modeling focusing on the release of phosphorus from sediments. To improve the simulation of the internal loading, the next step would be to collect data on resuspension of phosphorus from sediments. Furthermore, the lack of water quality data prevented extending the model outside of the simulated periods. The sources of uncertainty in the model are the accuracy of the water quality measurements, the manual calibration method used in this work, as well as the relative simplicity of the water quality module. In further work, modules that include zooplankton, different phytoplankton groups, and other variables (e.g., iron, silica, phosphorus fractions) can be tested to expand and enhance the model. The current model can assist water managers to plan mitigation strategies for the lake. The model can also be coupled with a hydrological water quality model of the catchment making it possible to examine socioeconomic projections by simulating future nutrient loading scenarios. Finally, while ecological models are typically developed using area-specific parameterization (Anagnostou et al., 2017), the major findings of this model agreed with those of other models from different regions indicating a wider applicability of the model following proper calibration.

5. Conclusions

A 3D hydrodynamic and eutrophication model was used in this study to reproduce algal blooms in Lake Vomb seen in the baseline year 2019, as well as to estimate eutrophication conditions in the year 2050 under two climate change scenarios, RCP4.5 and RCP8.5. The hydrodynamic model was shown to be effective in recreating lake water temperature. The model showed that Lake Vomb did not undergo stratification in 2019, whereas future scenarios predicted stronger vertical gradients in water temperature. The eutrophication model was adapted by modeling nutrients, dissolved oxygen, and biochemical oxygen demand processes. Cyanobacteria were successfully modeled in the lake represented by Chlorophyll-a. The model suggested that nitrogen levels in the lake were highly driven by external loading, but phosphorus levels in the lake were heavily impacted by internal loading via sediment release. According to future water quality predictions, Chlorophyll-a level is expected to rise up to 12% under warmer temperature conditions, regardless of external nutrient loading. Finally, uncertainties in the model range from the simplified description of processes to data availability and assumptions. This was the initial eutrophication model in Lake Vomb and therefore requires further improvement; nonetheless, the findings show that if no preventive management measures are taken, the lake will be susceptible to increasing harmful algal blooms in the future.

CRediT authorship contribution statement

Ahmed Elhabashy: Conceptualization, Methodology, Software, Writing – original draft, Visualization, Formal analysis. **Jing Li:** Conceptualization, Resources, Investigation, Writing – review & editing. **Ekaterina Sokolova:** Conceptualization, Resources, Writing – review & editing, Supervision, Funding acquisition.

Declaration of Competing Interest

The authors declare that they have no known competing financial interests or personal relationships that could have appeared to influence the work reported in this paper.

Data availability

Data will be made available on request.

Acknowledgements

This work was funded by the project ClimAQua (grant number 2017–01413 funded by Formas – the Swedish Research Council for Sustainable Development) and was conducted in cooperation with the project DiCyano (grant number 2020–03365 funded by VINNOVA – the Swedish Innovation Agency). We thank Dr. Jingjie Zhang for sharing modeling expertise and Brockmann Geomatics Sweden AB for providing satellite data. We also acknowledge the monitoring program at Lake Vomb by Sydvatten AB for the bathymetry and water temperature data.

Supplementary materials

Supplementary material associated with this article can be found, in the online version, at doi:10.1016/j.ecolmodel.2023.110275.

References

Anagnostou, E., Gianni, A., Zacharias, I., 2017. Ecological modeling and eutrophication—a review. Nat. Resour. Model. 30 (3), e12130. https://doi.org/10.1111/nrm.12130.

Bergion, V., Lindhe, A., Sokolova, E., Rosén, L., 2018. Risk-based cost-benefit analysis for evaluating microbial risk mitigation in a drinking water system. Water Res. 132, 111–123. https://doi.org/10.1016/j.watres.2017.12.054.

Chen, Y., Niu, Z., Zhang, H., 2013. Eutrophication assessment and management methodology of multiple pollution sources of a landscape lake in North China. Environ. Sci. Pollut. Res. 20 (6), 3877–3889. https://doi.org/10.1007/s11356-012-1331-0.

Chorus, I. & Welker, M. (2021). Toxic Cyanobacteria in water: a Guide to Their Public Health consequences, Monitoring and Management. (Chorus, I. & Welker, M., eds.) Second. Boca Raton: CRC Press /Tayldor & Francis Group.

Chuquimia, O.D., Bergion, V., Guzman-Otazo, J., Sörén, K., Rosén, L., Pettersson, T.J.R., Sokolova, E., Sjöling, Å., 2019. Molecular analyses of fecal bacteria and hydrodynamic modeling for microbial risk assessment of a drinking water source. Water (Basel) 12 (1), 3. https://doi.org/10.3390/w12010003.

Comber, S., Gardner, M., Darmovzalova, J., Ellor, B., 2015. Determination of the forms and stability of phosphorus in wastewater effluent from a variety of treatment processes. J. Environ. Chem. Eng. 3 (4), 2924–2930. https://doi.org/10.1016/j.jece.2015.10.002. Part A.

Conley, D.J., Paerl, H.W., Howarth, R.W., Boesch, D.F., Seitzinger, S.P., Havens, K.E., Lancelot, C., Likens, G.E., 2009. Controlling Eutrophication: nitrogen and Phosphorus. Science 323 (5917), 1014–1015. https://doi.org/10.1126/science.1167755.

Cornelissen, G., van Noort, P.C.M., Parsons, J.R., Govers, H.A.J., 1997. Temperature Dependence of Slow Adsorption and Desorption Kinetics of Organic Compounds in Sediments. Environ. Sci. Technol. 31 (2), 454–460. https://doi.org/10.1021/es960300+.

Cronberg, G., Annadotter, H., Lawton, L.A., 1999. The occurrence of toxic blue-green algae in Lake Ringsjön, southern Sweden, despite nutrient reduction and fish biomanipulation. Hydrobiologia 404 (0), 123–129. https://doi.org/10.1023/A:1003780731471.

Cui, Y., Zhu, G., Li, H., Luo, L., Cheng, X., Jin, Y., Trolle, D., 2016. Modeling the response of phytoplankton to reduced external nutrient load in a subtropical Chinese reservoir using DYRESM-CAEDYM. Lake Reserv Manag 32 (2), 146–157. https://doi.org/10.1080/10402381.2015.1136365.

Ekologigruppen Ekoplan A.B. (2020). *Kävlingeån Water Control (Kävlingeån Vattenkontroll* 2019*)*. http://www.xn–kvlingen-0zaq.se/wp-content/uploads/2021/12/K%C3%A4vlinre%C3%A5n_recipientkontroll-2019_updaterad.pdf.

Ekologigruppen Ekoplan A.B. (2021). *Kävlingeån Water Control (Kävlingeån Vattenkontroll 2020)*. http://www.xn–kvlingen-0zaq.se/wp-content/uploads/2021/12/K%C3%A4vlinge%C3%A5n_recipientkontroll-2020.pdf.

Elliott, J.A., Defew, L., 2012. Modelling the response of phytoplankton in a shallow lake (Loch Leven, UK) to changes in lake retention time and water temperature. Hydrobiologia 681 (1), 105–116. https://doi.org/10.1007/s10750-011-0930-y.

Elliott, J.A., Persson, I., Thackeray, S.J., Blenckner, T., 2007. Phytoplankton modelling of Lake Erken, Sweden by linking the models PROBE and PROTECH. Ecol. Modell. 202 (3), 421–426. https://doi.org/10.1016/j.ecolmodel.2006.11.004.

Erisman, J.W., Galloway, J.N., Seitzinger, S., Bleeker, A., Dise, N.B., Petrescu, A.M.R., Leach, A.M., de Vries, W., 2013. Consequences of human modification of the global nitrogen cycle. Philosophical Trans. Royal Society B: Biol. Sci. 368 (1621), 20130116 https://doi.org/10.1098/rstb.2013.0116.

Freeman, E.C., Creed, I.F., Jones, B., Bergström, A.-K., 2020. Global changes may be promoting a rise in select cyanobacteria in nutrient-poor northern lakes. Glob. Chang Biol. 26 (9), 4966–4987. https://doi.org/10.1111/gcb.15189.

Guven, B., Howard, A., 2006. A review and classification of the existing models of cyanobacteria. Progress in Phys. Geography: Earth and Environ. 30 (1), 1–24. https://doi.org/10.1191/0309133306pp464ra.

Huang, J., Xu, Q., Wang, X., Xi, B., Jia, K., Huo, S., Liu, H., Li, C., Xu, B., 2015. Evaluation of a modified monod model for predicting algal dynamics in Lake Tai. Water (Basel) 7 (7), 3626–3642. https://doi.org/10.3390/w7073626.

Huisman, J., Codd, G.A., Paerl, H.W., Ibelings, B.W., Verspagen, J.M.H., Visser, P.M., 2018. Cyanobacterial blooms. Nat. Rev. Microbiol. 16 (8), 471–483. https://doi.org/10.1038/s41579-018-0040-1.

Jiménez-Navarro, I.C., Jimeno-Sáez, P., López-Ballesteros, A., Pérez-Sánchez, J., Senent-Aparicio, J., 2021. Impact of climate change on the hydrology of the forested watershed that drains to Lake Erken in Sweden: an analysis using SWAT+ and CMIP6 scenarios. Forests 12 (12), 1803. https://doi.org/10.3390/f12121803.

Johansson, E., Legrand, C., Björnerås, C., Godhe, A., Mazur-Marzec, H., Säll, T., Rengefors, K., 2019. High diversity of microcystin chemotypes within a summer bloom of the cyanobacterium microcystis botrys. Toxins (Basel) 11 (12), 698. https://doi.org/10.3390/toxins11120698.

Kakouei, K., Kraemer, B.M., Anneville, O., Carvalho, L., Feuchtmayr, H., Graham, J.L., Higgins, S., Pomati, F., Rudstam, L.G., Stockwell, J.D., Thackeray, S.J., Vanni, M.J., Adrian, R., 2021. Phytoplankton and cyanobacteria abundances in mid-21st century lakes depend strongly on future land use and climate projections. Glob. Chang. Biol. 27 (24), 6409–6422. https://doi.org/10.1111/gcb.15866.

Li, J., Hansson, L.-A., Persson, K.M., 2018. Nutrient control to prevent the occurrence of cyanobacterial blooms in a Eutrophic Lake in Southern Sweden, used for drinking water supply. Water (Basel) 10 (7), 919. https://doi.org/10.3390/w10070919.

Li, Y., Zhang, Q., Zhang, L., Tan, Z., Yao, J., 2017. Investigation of Water Temperature Variations and Sensitivities in a Large Floodplain Lake System (Poyang Lake, China) Using a Hydrodynamic Model. Remote Sensing 9 (12), 1231. https://doi.org/10.3390/rs9121231.

Markensten, H., Moore, K., Persson, I., 2010. Simulated lake phytoplankton composition shifts toward cyanobacteria dominance in a future warmer climate. Ecol. App. 20 (3), 752–767. https://doi.org/10.1890/08-2109.1.

Meerhoff, M., Audet, J., Davidson, T.A., De Meester, L., Hilt, S., Kosten, S., Liu, Z., Mazzeo, N., Paerl, H., Scheffer, M., Jeppesen, E., 2022. Feedback between climate change and eutrophication: revisiting the allied attack concept and how to strike

back. Inland Waters 12 (2), 187–204. https://doi.org/10.1080/20442041.2022.2029317.
Méjean, A., Paci, G., Gautier, V., Ploux, O., 2014. Biosynthesis of anatoxin-a and analogues (anatoxins) in cyanobacteria. Toxicon 91, 15–22. https://doi.org/10.1016/j.toxicon.2014.07.016.
Motew, M., Chen, X., Booth, E.G., Carpenter, S.R., Pinkas, P., Zipper, S.C., Loheide, S.P., Donner, S.D., Tsuruta, K., Vadas, P.A., Kucharik, C.J., 2017. The influence of legacy p on lake water quality in a midwestern agricultural watershed. Ecosystems 20 (8), 1468–1482. https://doi.org/10.1007/s10021-017-0125-0.
Paerl, H.W., Barnard, M.A., 2020. Mitigating the global expansion of harmful cyanobacterial blooms: moving targets in a human- and climatically-altered world. Harmful Algae 96, 101845. https://doi.org/10.1016/j.hal.2020.101845.
Payen, S., Cosme, N., Elliott, A.H., 2021. Freshwater eutrophication: spatially explicit fate factors for nitrogen and phosphorus emissions at the global scale. Int. J. Life Cycle Assess. 26 (2), 388–401. https://doi.org/10.1007/s11367-020-01847-0.
Piccolroaz, S., Woolway, R.I., Merchant, C.J., 2020. Global reconstruction of twentieth century lake surface water temperature reveals different warming trends depending on the climatic zone. Clim. Change 160 (3), 427–442. https://doi.org/10.1007/s10584-020-02663-z.
Qin, B., Zhou, J., Elser, J.J., Gardner, W.S., Deng, J., Brookes, J.D., 2020. Water depth underpins the relative roles and fates of nitrogen and phosphorus in lakes. Environ. Sci. Technol. 54 (6), 3191–3198. https://doi.org/10.1021/acs.est.9b05858.
Redshaw, C.J., Mason, C.F., Hayes, C.R., Roberts, R.D., 1990. Factors influencing phosphate exchange across the sediment-water interface of eutrophic reservoirs. Hydrobiologia 192 (2), 233–245. https://doi.org/10.1007/BF00006018.
Schindler, D.W., Carpenter, S.R., Chapra, S.C., Hecky, R.E., Orihel, D.M., 2016. Reducing phosphorus to curb lake eutrophication is a success. Environ. Sci. Technol. 50 (17), 8923–8929. https://doi.org/10.1021/acs.est.6b02204.
Taranu, Z.E., Gregory-Eaves, I., Leavitt, P.R., Bunting, L., Buchaca, T., Catalan, J., Domaizon, I., Guilizzoni, P., Lami, A., McGowan, S., Moorhouse, H., Morabito, G., Pick, F.R., Stevenson, M.A., Thompson, P.L., Vinebrooke, R.D., 2015. Acceleration of cyanobacterial dominance in north temperate-subarctic lakes during the Anthropocene. Ecol. Lett. 18 (4), 375–384. https://doi.org/10.1111/ele.12420.
Tasnim, B., Fang, X., Hayworth, J.S., Tian, D., 2021. Simulating nutrients and phytoplankton dynamics in lakes: model development and applications. Water (Basel) 13 (15), 2088. https://doi.org/10.3390/w13152088.
Thomas, M.K., Aranguren-Gassis, M., Kremer, C.T., Gould, M.R., Anderson, K., Klausmeier, C.A., Litchman, E., 2017. Temperature–nutrient interactions exacerbate sensitivity to warming in phytoplankton. Glob. Chang. Biol. 23 (8), 3269–3280. https://doi.org/10.1111/gcb.13641.
Trolle, D., Hamilton, D.P., Pilditch, C.A., Duggan, I.C., Jeppesen, E., 2011. Predicting the effects of climate change on trophic status of three morphologically varying lakes: implications for lake restoration and management. Environ. Modell. Software 26 (4), 354–370. https://doi.org/10.1016/j.envsoft.2010.08.009.
Trolle, D., Jørgensen, T.B., Jeppesen, E., 2008. Predicting the effects of reduced external nitrogen loading on the nitrogen dynamics and ecological state of deep Lake Ravn, Denmark, using the DYRESM–CAEDYM model. Limnologica 38 (3), 220–232. https://doi.org/10.1016/j.limno.2008.05.009.
Vinçon-Leite, B., Casenave, C., 2019. Modelling eutrophication in lake ecosystems: a review. Sci. Total Environ. 651, 2985–3001. https://doi.org/10.1016/j.scitotenv.2018.09.320.
Willén, T., 1972. The gradual destruction of Sweden's Lakes. Ambio 1 (1), 6–14.
Willén, E., 2001. Phytoplankton and Water Quality Characterization: experiences from the Swedish Large Lakes Mälaren, Hjälmaren, Vättern and Vänern. AMBIO: A J. Human Environ. 30 (8), 529–537. https://doi.org/10.1579/0044-7447-30.8.529.
Wu, Y., Wen, Y., Zhou, J., Wu, Y., 2014. Phosphorus release from lake sediments: effects of pH, temperature and dissolved oxygen. KSCE J. Civil Eng. 18 (1), 323–329. https://doi.org/10.1007/s12205-014-0192-0.
Xie, L., Hagar, J., Rediske, R.R., O'Keefe, J., Dyble, J., Hong, Y., Steinman, A.D., 2011. The influence of environmental conditions and hydrologic connectivity on cyanobacteria assemblages in two drowned river mouth lakes. J. Great Lakes Res. 37 (3), 470–479. https://doi.org/10.1016/j.jglr.2011.05.002.
Yindong, T., Xiwen, X., Miao, Q., Jingjing, S., Yiyan, Z., Wei, Z., Mengzhu, W., Xuejun, W., Yang, Z., 2021. Lake warming intensifies the seasonal pattern of internal nutrient cycling in the eutrophic lake and potential impacts on algal blooms. Water Res. 188, 116570 https://doi.org/10.1016/j.watres.2020.116570.